



ELSEVIER

Thermochimica Acta 287 (1996) 81–90

thermochimica
acta

Thermal decomposition study of $[\text{MCu}(\text{C}_3\text{H}_2\text{O}_4)_2(\text{H}_2\text{O})_n]$ phases (M is Ca ($n = 3$), Sr and Ba ($n = 4$))

M. Insausti^a, I. Gil de Muro^a, L. Lorente^a, T. Rojo^{a,*}
E.H. Bocanegra^b, M.I. Arriortua^c

^a Departamento de Química Inorgánica, Universidad del País Vasco, Apdo. 644, 48080, Bilbao, Spain

^b Departamento de Física Aplicada II, Universidad del País Vasco, Apdo. 644, 48080, Bilbao, Spain

^c Departamento de Mineralogía-Petrología, Universidad del País Vasco, Apdo. 644, 48080, Bilbao, Spain

Received 10 February 1996; accepted 22 March 1996

Abstract

Three new compounds with the general formula $[\text{MCu}(\text{C}_3\text{H}_2\text{O}_4)_2(\text{H}_2\text{O})_n]$ (M is Ca ($n = 3$), Sr and Ba ($n = 4$)) have been synthesized and characterized by analytical and infrared techniques. X-ray diffraction methods have shown that all the complexes have orthorhombic unit cells. Thermal decomposition of these compounds using TGA–DSC and DTA techniques involves three consecutive steps: dehydration, ligand pyrolysis and inorganic residue evolution. Dehydration is an endothermic process with enthalpies of around 200 kJ mol^{-1} . Kinetic analysis of the dehydration curves has been performed and the Johnson equation gave the best correlation factors for the three complexes. Further treatments in tubular furnaces resulted in the formation of mixed oxides of formula MCuO_2 (M is Ca, Sr and Ba). The formation of small homogeneous particles in these oxides, as with metallo-organic precursors, has been observed by scanning electron microscopy.

Keywords: Alkaline-earth and copper malonates; DTA; Mixed oxides; TGA

1. Introduction

MCuO_2 (M is Ca, Sr, Ba) phases represent a group of oxocuprates closely related to the high- T_c superconductors [1]. Thus, a detailed understanding of their magnetic and structural properties is of great interest. Moreover, it has been established that the methods of preparation play a very important role in the properties of the solids,

* Corresponding author.

especially when the compounds are obtained at low temperatures [2]. The majority of the earlier studies on oxocuprates involved preparative reactions based on conventional solid state reactions. In recent years, alternative syntheses have been used [3] in an attempt to avoid the limitations of this method.

Bimetallic precursors with the same metal stoichiometry as the target oxides are of particular interest, since these, in principle, should give the most homogeneous stoichiometric products and lower processing temperatures [4]. Several studies have been performed using different carboxylates as binding agents in the metallo-organic precursors [5,6]. Among these carboxylates, the use of malonic acid, with small amounts of carbon that are removed in the decomposition process, could lead to the required oxides [7].

For this reason, we have focused this work on the preparation of complexes with the formula $[\text{MCu}(\text{C}_3\text{H}_2\text{O}_4)_2(\text{H}_2\text{O})_n]$; M is Ca ($n = 3$), Sr ($n = 4$), and Ba ($n = 4$). In order to determine the influence of the temperature at which the complexes decompose, as well as the stages implied in the process, a detailed thermal study was undertaken. In addition, a comparative study of the different methods for obtaining these oxides, related to the morphology of the final products, will be performed.

2. Experimental

2.1. Materials

The compounds were prepared by adding 0.242 g (2 mmol) of copper nitrate to an aqueous solution of 2 mmol of sodium malonate. After leaving for two hours to ensure total complexation, 1 mmol of the corresponding alkaline-earth metal chloride in aqueous solution was added in each case. For strontium and barium, crystalline blue precipitates were immediately obtained. Single crystals were prepared by filtration. For the calcium compound, pale blue crystals were obtained after two days. The crystals and powder were filtered, washed with water and acetone, and dried over P_2O_5 . In this way, the following complexes were obtained: $[\text{CaCu}(\text{C}_3\text{H}_2\text{O}_4)_2(\text{H}_2\text{O})_3]$, $[\text{SrCu}(\text{C}_3\text{H}_2\text{O}_4)_2(\text{H}_2\text{O})_4]$ and $[\text{BaCu}(\text{C}_3\text{H}_2\text{O}_4)_2(\text{H}_2\text{O})_4]$.

2.2. Measurements

C and H contents were determined by elemental analysis and metals by atomic absorption spectroscopy (Table 1).

Infrared spectra were recorded on a Mattson FTIR 1000 spectrophotometer using KBr discs (2%). TG and DSC curves obtained using a Perkin-Elmer System-7 DSC–TGA unit at a heating rate of $10^\circ\text{C min}^{-1}$ in flowing atmospheres of N_2 and air. DTA curves were recorded in a Setaram DTA92 system at the same heating rate in following argon. About 25 mg of powdered sample, in a platinum pan, was used in each experiment.

X-ray powder diffraction patterns of the final products were obtained by means of a STOE Diffractometer equipped with a germanium monochromator using $\text{Cu K}\alpha_1$

Table 1
Analytical data of the complexes

Compound	Found (calculated) %			
	C	H	Cu	M(Ca, Sr, Ba)
CaCuC ₆ H ₁₀ O ₁₁	19.12 (19.92)	2.86 (2.78)	18.06 (17.56)	10.06 (11.07)
SrCuC ₆ H ₁₂ O ₁₂	16.97 (17.60)	2.64 (2.95)	14.65 (15.52)	20.86 (21.40)
BaCuC ₆ H ₁₂ O ₁₂	15.13 (15.70)	2.43 (2.63)	12.92 (13.84)	29.28 (29.91)

radiation. In order to compare the different patterns, Journal of Powder Diffraction Files (JCPDS) and theoretical generated diagrams were used.

Morphologies of the final oxides were observed by scanning microscopy in a JEOL JSM-6400, operating at 20 keV, the samples having been coated with gold by d.c. sputtering (BAL-TEC SCD 004 Sputter Coater).

2.3. Kinetic treatment

The kinetic analysis was carried out via the TG curves recorded at a constant heating rate, $\beta = dT/dt$. Taking into account the Arrhenius equation, the expression

$$g(x) = kt \quad (1)$$

becomes

$$g(x) = k dt = \frac{AE_a}{\beta R} P(x) \quad (2)$$

where $x = E_a/RT$ and $g(x)$ is a function depending on the actual kinetic law. It is based on the rapid convergence of the $P(x)$ function. After taking logarithms and regrouping terms, Eq. (2) can be written as

$$\log(g(x)) - \log(p(x)) = \log \frac{AE_a}{\beta R} \quad (3)$$

which is known as Satava's integral method [8].

All data were transferred to a computer and linear plots were drawn for the general solid state rate expressions of $\log(g(x))$ vs. $1/T$ by the least-squares method. E_a , A and the corresponding correlation coefficients for the linear plots were calculated. In this way, coefficients closest to unity were selected.

3. Results and discussion

3.1. Crystal data

Blue rhombic crystal were obtained and crystal data determined from Weissenberg photographs with Cu K α radiation for all compounds. Final cell parameters were

obtained by least squares refinement, LSUCRE [9], of indexed powder diffraction patterns (Table 2). The structural determination is currently being performed.

3.2. IR spectra

The more characteristic bands of the infrared spectra for the ligand and the complexes are reported in Table 3.

All compounds showed a strong, broad absorption band in the region 3500–3300 cm^{-1} , $\nu(\text{O}-\text{H})$, indicating the presence of water molecules.

In these dicarboxylates, the frequencies of most interest with regard to the structures are those of the C–O vibrations. The IR spectra of the malonic acid show a $\nu_{\text{asym}}(\text{OCO})$ peak in the vicinity of 1700 cm^{-1} , which is indicative of free carboxyl groups [10].

In this complexes, this $\nu_{\text{asym}}(\text{OCO})$ band is shifted to a lower frequency, showing that complexation is carried out through the carbonyl group. The $\nu_{\text{sym}}(\text{OCO})$ band in the complexes was observed at about 1400 cm^{-1} . The decrease in the difference ($\Delta\nu$) between $\nu_{\text{asym}}(\text{OCO})$ and $\nu_{\text{sym}}(\text{OCO})$ in the complexes has been taken as a measure of the M–O bond [10]. The lowering of both $\nu(\text{OCO})$ frequencies is due to the drainage of the electron density from the carboxylate group to the metal, forming chelates or bridges between the carboxylates. The splitting of the band corresponding to the

Table 2
Refined cell parameters of the different complexes

Compound	[CaCu(C ₃ H ₂ O ₄) ₂ (H ₂ O) ₃]	[SrCu(C ₃ H ₂ O ₄) ₂ (H ₂ O) ₄]	[BaCu(C ₃ H ₂ O ₄) ₂ (H ₂ O) ₄]
<i>a</i> /Å	6.810(1)	6.73(1)	6.85(2)
<i>b</i> /Å	16.370(1)	18.86(2)	18.2(3)
<i>c</i> /Å	9.480(1)	9.262(4)	9.38(3)
Laue group	mmm	mmm	mmm

Table 3
Characteristic bands in the infrared spectra (3500–400 cm^{-1})

Compounds	$\nu(\text{O}-\text{H})$	$\nu(\text{C}-\text{H})$	$\nu_{\text{asym}}(\text{C}-\text{O})$	$\nu_{\text{sym}}(\text{C}-\text{O})$	$\nu(\text{M}-\text{O})$
Malonic acid	3580– 3300	2960	1730	1388 1330	–
CaCu(C ₃ H ₂ O ₄) ₂ (H ₂ O) ₃	3500– 3350	2920 2850	1590	1450 1370	590 550
SrCu(C ₃ H ₂ O ₄) ₂ (H ₂ O) ₄	3448	3050 2935	1590 1567	1446 1380	587 554
BaCu(C ₃ H ₂ O ₄) ₂ (H ₂ O) ₄	3400	3030 2930	1600 1570	1438 1380	630 553

carboxylate group could be indicative of both types of bonding. The bands which appear around 600 cm^{-1} are associated with the M–O vibrations.

3.3. Thermal analysis

The TG–DTA curves of the three complexes in flowing air atmosphere are shown in Figs. 1 and 2. The decomposition patterns obtained from the TG curves present three consecutive stages: dehydration, ligand pyrolysis and evolution of the inorganic residue, leading to a residual weight corresponding to metal oxides.

Dehydration

Thermal decomposition starts with the loss of the water molecules. The observed weight losses of the process compare favourably with the theoretical values summarized in Table 4. The calorimetric measurements (Fig. 3) show the decomposition stages as sharp endothermic peaks, from which the dehydration enthalpies were calculated. These values are of the same magnitude as those previously obtained for other metallo-organic complexes [11]. For the strontium compound, a slight splitting of the dehydration peak in the DSC curve is observed, which could be indicative of different water molecules in the cell. Nevertheless, only one step appears for the calcium and barium compounds. All these expected endothermic peaks have also been observed in the DTA curves.

Kinetic analysis of the dehydration curves was first performed using Satava's integral method [8]. Comparison of the fit to the various kinetic equations (those commonly used in kinetic analysis for solid state reactions) showed that the best fit to

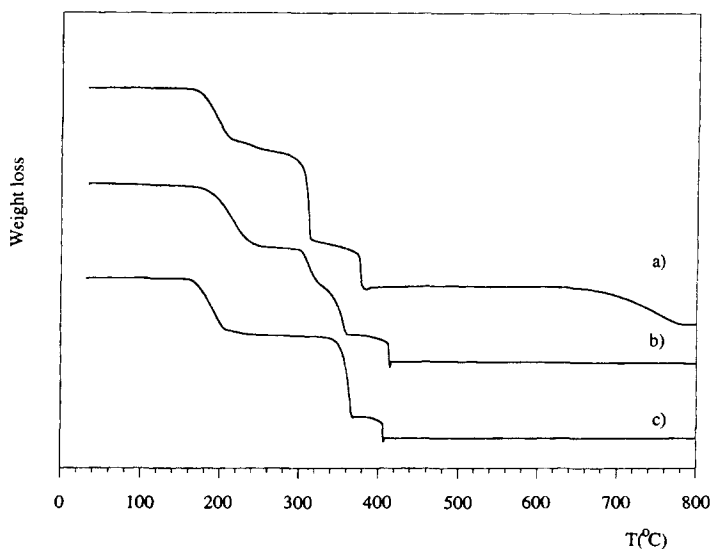


Fig. 1. TG curves for the (a) $\text{CaCu}(\text{C}_3\text{H}_2\text{O}_4)_2(\text{H}_2\text{O})_3$, (b) $\text{SrCu}(\text{C}_3\text{H}_2\text{O}_4)_2(\text{H}_2\text{O})_4$ and (c) $\text{BaCu}(\text{C}_3\text{H}_2\text{O}_4)_2(\text{H}_2\text{O})_4$ complexes in air atmosphere.

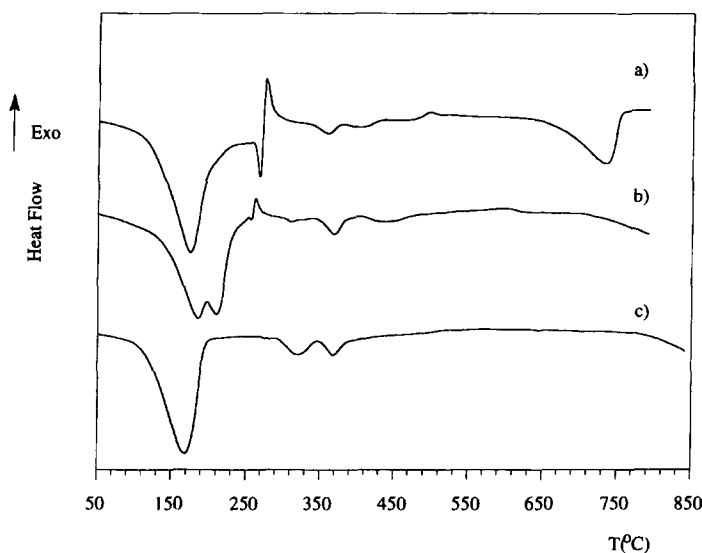


Fig. 2. DTA curves for the (a) $\text{CaCu}(\text{C}_3\text{H}_2\text{O}_4)_2(\text{H}_2\text{O})_3$, (b) $\text{SrCu}(\text{C}_3\text{H}_2\text{O}_4)_2(\text{H}_2\text{O})_4$ and (c) $\text{BaCu}(\text{C}_3\text{H}_2\text{O}_4)_2(\text{H}_2\text{O})_4$ complexes in argon atmosphere.

Table 4

Thermal analysis data of the dehydration steps of $[\text{MCu}(\text{C}_3\text{H}_2\text{O}_4)_2(\text{H}_2\text{O})_n]$ (M is Ca ($n = 3$), Sr and Ba ($n = 4$))

Compound	H_2O molecules	Range $T/^\circ\text{C}$	Weight losses (%)		Kinetic equation ^a	E_a (kJ mol^{-1})	$\Delta H/$ (kJ mol^{-1})
			Exp.	Theor.			
$\text{CaCu}(\text{mal})_2(\text{H}_2\text{O})_3$	3	186–273	15.6	15.9	JE	200	149
$\text{SrCu}(\text{mal})_2(\text{H}_2\text{O})_4$	4	192–245	17.0	17.6	JE	168	294
$\text{BaCu}(\text{mal})_2(\text{H}_2\text{O})_4$	4	156–252	15.0	15.8	JE	179	205

^a JE, Johnson equation: $g(\alpha) = \frac{1}{1 - \alpha} - 1$.

the data was obtained with the Johnson equation (Table 4). The activation energy values are similar to those observed in other measurements of malonato complexes [12], in this case the calcium compound showing the maximum value.

Ligand pyrolysis

After the stability interval following dehydration, the compounds undergo ligand pyrolysis (290–410°C), which takes place in at least two main steps. In the first, the weight loss observed corresponds to both the decomposition of the malonato ligand and the formation of the carbonates and oxocarbonates of the metals. Nevertheless,

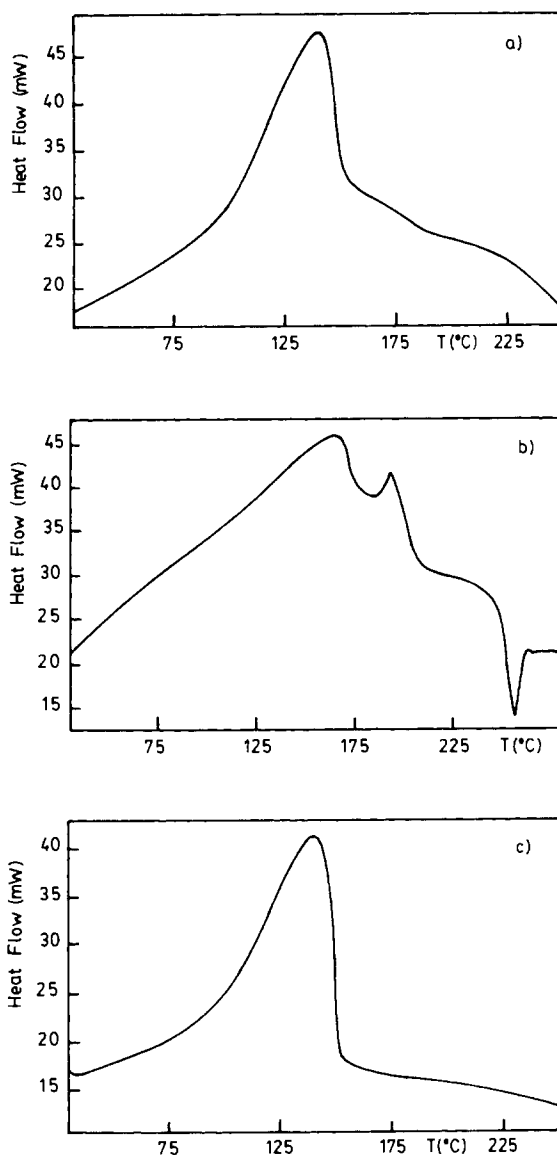


Fig. 3. DSC curves for the dehydration step of the (a) $\text{CaCu}(\text{C}_3\text{H}_2\text{O}_4)_2(\text{H}_2\text{O})_3$, (b) $\text{SrCu}(\text{C}_3\text{H}_2\text{O}_4)_2(\text{H}_2\text{O})_4$ and (c) $\text{BaCu}(\text{C}_3\text{H}_2\text{O}_4)_2(\text{H}_2\text{O})_4$ complexes.

unstable copper carbonates decompose around 350°C and yield CuO . Then a small increase in the weight is observed at 410°C for the strontium and barium compounds, and at 390°C for the calcium complex. This result is due to the oxidation of small quantities of Cu_2O and metallic copper to CuO , which are also produced in the decomposition process [13]. In the DTA curves, small exothermic peaks appear which

are associated with this process. In this way, ligand pyrolysis finishes with a stable step which fits well with a mixture of the alkaline-earth carbonate and CuO.

Inorganic residue evolution

An understanding of the evolution that the inorganic residue undergoes is required for the study of the final products.

For the calcium compound, the stable step finished at 660°C, where decarbonation occurs, as can be deduced from the weight loss observed. At this temperature, a broad endothermic peak associated with this process can be observed in the DTA curve. X-ray diffraction analysis of the residue confirms the above results and a mixture of CuO, CaO, $\text{Ca}_{1-x}\text{CuO}_2$ [14] and Ca_2CuO_3 oxides is obtained. The heating rate ($10^\circ\text{C min}^{-1}$) does not allow the formation of a single, pure oxide. For the strontium and barium compounds, the thermogravimetric curve finishes at 800°C and decarbonation has not occurred. In the DTA curves, performed up to 850°C, the continuous decrease in the heat flow at these temperatures can be explained by the beginning of the decarbonation process in both compounds.

In order to obtain pure phases of the MCuO_2 oxides (M is Ca, Sr, Ba) from the complexes, they were heated in tubular furnaces at several temperatures and in air atmosphere, and the resulting products characterized by X-ray powder diffraction. Scanning electron microscopy was used to study the morphology of the final products. In order to decompose the organic part, all the complexes were previously fired at 400°C.

In the case of the $[\text{CaCu}(\text{C}_3\text{H}_2\text{O}_4)_2(\text{H}_2\text{O})_3]$ compound, at 600°C the $\text{Ca}_{1-x}\text{CuO}_2$ phase was obtained but impurities corresponding to CuO and CaO appeared. Three hours at 650°C was enough to obtain the non-stoichiometric $\text{Ca}_{1-x}\text{CuO}_2$ phase, with some CaO. Similar results have been obtained in the decomposition of other complexes with calcium [5,6,15], in contrast with the long reaction times and high temperatures required for the formation of the mixed oxide by the ceramic method [14].

For the $[\text{SrCu}(\text{C}_3\text{H}_2\text{O}_4)_2(\text{H}_2\text{O})_4]$ compound, a thermal treatment of 3 h at 800°C was necessary to decompose all the carbonates to obtain the SrCuO_2 oxide. However, for the barium compound, 10 h were needed to decompose the carbonate at 800°C, due to the increasing stability of the carbonates down the group.

The above results can be compared with those obtained in other investigations, not only with this kind of ligand [5,6] but also using other synthesis methods, such as sol-gel techniques. It can be deduced that in all cases the oxides obtained from the metallo-organic precursors have been prepared at relatively short times and temperatures, compared with the ceramic method, although the combustion of the polymers needs some time.

Finally, the influence of these decomposition methods on the final grain size has been analysed by SEM. The photographs observed in Fig. 4 correspond to the calcium, strontium and barium oxides. The microstructure reveals uniform, fine prismatic particles, owing to the gentle decomposition from the metallo-organic precursors. In this way, the uniform particle size obtained provides a measure of the stability of these compounds against the exaggerated grain growth observed in the ceramic method [16]. In some cases, the small size of the particles leads to the start of a sintering process, as noted by the formation of small 'necks' between the particles.

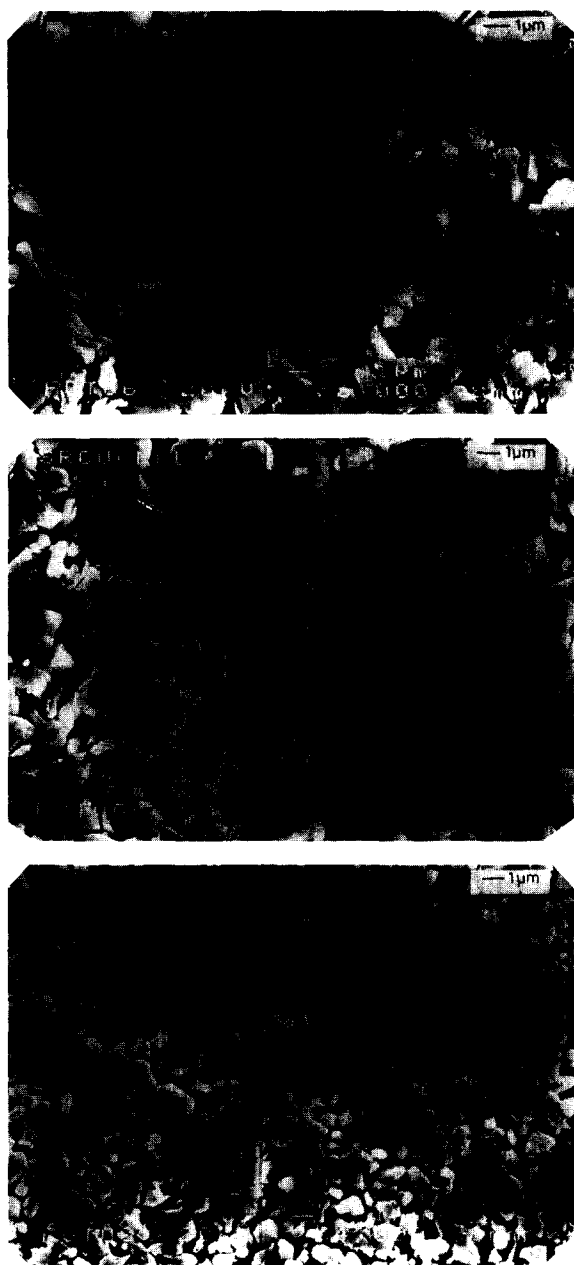


Fig. 4. SEM micrographs of the (a) $\text{Ca}_{1-x}\text{CuO}_2$, (b) SrCuO_2 and (c) BaCuO_2 powders.

Acknowledgement

This work was financially supported by the DGICYT (PB94-0469) and the Spanish-German Cooperation project (n°41).

References

- [1] H. Müller-Buschbaum, *Ang. Chem. Ed. Engl.*, 30 (1991) 723.
- [2] S. Sundar Manoharan and K.C. Patil, *J. Solid State Chem.*, 102 (1993) 267.
- [3] J. Gopalakrishnan, *Chem. Mater.*, 7(7) (1995) 1265.
- [4] K.G. Caulton and L.G. Hubert-Pfalzgraf, *Chem. Rev.*, 90 (1990) 969.
- [5] M. Insausti, R. Cortés, M.I. Arriortua, T. Rojo and E.H. Bocanegra, *Solid State Ionics*, 63–65 (1993) 351.
- [6] M. Insausti, L.J. Pizarro, L. Lezama, R. Cortés, E.H. Bocanegra, M.I. Arriortua, and T. Rojo, *Chem. Mater.*, 6(5) (1994) 707.
- [7] J.R. Allan, B.R. Carson, D.L. Gerrard and S. Hoey, *Thermochim. Acta*, 147 (1989) 353.
- [8] V. Satava, *Thermochim. Acta*, 2 (1971) 423.
- [9] D.E. Appleman and H.T. Evans, *LSUCRE, Indexing and Least-Squares Refinement of Powder Diffraction Data*, Report PB-216188, U.S. Dept. of Commerce, N.T.I.S., 5285, Port Royal Rd., Springfield, VA22151, 1973.
- [10] K. Nakamoto, *Infrared spectra of Inorganic and Coordination Compounds*, 4th edn., John Wiley and Sons, New York, 1986.
- [11] T. Rojo, M. Insausti, M.I. Arriortua, E. Hernández and J. Zubillaga, *Thermochim. Acta*, 195 (1992) 95.
- [12] H.L. Saha and S. Mitra, *Thermochim. Acta*, 112 (1987) 275.
- [13] R. Mehrotra and R. Bohra, *Metal Carboxilates*, Academic Press, London, 1983.
- [14] R.S. Roth, N.M. Hwang, J.R. Claudia, P.B. Burton and J.J. Ritter, *J. Am. Ceram. Soc.*, 74(9) (1991) 2148.
- [15] M.J. Sanchis, F. Sapiña, R. Ibáñez, A. Beltrán and D. Beltrán, *Mater. Lett.*, 12 (1992) 409.
- [16] F.F. Lange, in L.L. Hench and J.K. West (Eds.), *Chemical Processing of Advanced Materials*, John Wiley and Sons, New York, 1992.